CCFE-PR(15)17

J.R. Harrison, G.M. Fishpool, B.D. Dudson

Filamentary Transport in the Private Flux Region in MAST

Filamentary Transport in the Private Flux Region in MAST

J.R. Harrison[1], G.M. Fishpool[1], B.D. Dudson[2]

[1]CCFE, Culham Science Centre, Abingdon, Oxfordshire, OX14 3DB, UK.
[2]York Plasma Institute, Department of Physics, University of York, Heslington, York, YO10 5DD, UK

The following article was subsequently published in Plasma-Surface Interactions 21. Proceedings of the 21st International Conference on Plasma-Surface Interactions in Controlled Fusion Devices, Kanazawa, Japan. May 26-30, 2014. Journal of Nuclear Materials, Vol.463, August 2015, pp.757-760

Filamentary Transport in the Private Flux Region in MAST and Correlation with Density e-Folding Widths

J. R. Harrison[a], G. M. Fishpool[a], B. D. Dudson[b], A. Kirk

[a] *CCFE, Culham Science Centre, Abingdon, OX14 3DB, UK*

[b] *York Plasma Institute, Department of Physics, University of York, Heslington, York, YO10 5DD, UK*

Abstract

Measurements of light fluctuations within the divertor volume of MAST provide strong evidence for the existence of filamentary structures within the private flux region (PFR). These filaments are observed in L-mode and H-mode confinement regimes. Correlation analysis of the camera data has been used to confirm the hypothesis that the filaments observed in the line integrated camera data are genuinely within the PFR. Fluctuations at a given location in the PFR in the image are strongly correlated with fluctuations at other locations within the PFR where connected by field lines. The region of most concentrated light emission from the filamentary structure is generally close to the separatrix on the inner leg and moves with time towards the inner divertor target, whilst plasma is seen to be ejected deeper into the PFR away from the separatrix.

PACS: 52.35.Ra, 52.55.Fa

PSI-21 keywords: MAST, Visible imaging, Boundary transport, Non-diffusive transport

**Corresponding author address:* Culham Centre for Fusion Energy, Culham Science Centre, Abingdon, OX14 3DB, UK

**Corresponding author E-mail:* james.harrison@ccfe.ac.uk

Presenting author: James Harrison

Presenting author email: james.harrison@ccfe.ac.uk

1. Introduction

When extrapolating data from existing machines to predict the divertor heat loads in larger devices such as ITER, gaps in our understanding of transport processes parallel and perpendicular to field lines can be a large source of uncertainty. To this end, it is important to understand the *nature* of cross-field transport, i.e. convective, diffusive or a combination. For the transport of particles into the private flux region (PFR), it is sometimes effectively assumed that diffusion transports particles and heat from the scrape-off layer [1, 2]. Recent observations of light fluctuations in the divertor volume in MAST have provided strong evidence for the existence of filamentary structures occurring within the private flux region (PFR), suggesting that convection plays a role in the transport. The observation of intermittent transport in the private flux region is supported by measurements of ion saturation current fluctuations at the inner divertor target of JET [3] and MAST pdudsonerf], suggesting the presence of strong fluctuations, of order 15% of the mean value, in both the SOL and PFR sides of the separatrix. Furthermore, modelling studies using BOUT [4, 6] and analytic studies [7] predicted that fluctuations should occur in the bad curvature region of the PFR of the inner leg. The camera measurements and general observations of fluctuations in the divertor are presented in section 2. In section 3, results of correlation analysis of the fluctuations in the PFR are shown. A qualitative description is presented in section 4, followed by a discussion and summary in section 5.

2. Measurements of Divertor Fluctuations

Line integrated measurements of light fluctuations within the divertor were made using a Photron SA1.1 camera operated at 120kHz and a lens assembly that allowed for full coverage of the divertor at a spatial resolution of 6mm at the tangency plane. An illustration of the region viewed by the camera and a raw image are shown in Figure 1. The data presented in this paper were acquired from an inter-ELM H-mode period in MAST shot 29564 (0.406-0.414s), a pulse with 620kA plasma current, core density $4x10^{19}m^{-3}$ and 1.2MW of NBI heating. The plasma was down-shifted into a lower single-null configuration, which is optimal for divertor imaging diagnostics. The data presented are representative of typical MAST discharges, both L- and H- mode, and the observations are not specific to this shot.

To emphasise the filament dynamics, a moving average background subtraction is applied to the raw data and the image subsequently contrast enhanced using the Spiceweasel code [spiceweaselref]. An output from the code applied to this data is shown in Figure 2 (left image), clearly showing a variety of field-aligned fluctuations in several areas of the image. Observations from L-mode and H-mode discharges suggest that there appear to be three types of fluctuations that occur within the divertor. Firstly, filaments in the scrape-off layer, originating upstream and becoming highly elongated due to the strong shear near the X-point [5]. Secondly, there are high frequency (several 10's of kHz) fluctuations of ~1cm extent localised to a region very close to the separatrix. Lastly, there are filaments that appear brightest in the private flux region of the inner divertor leg, appearing to move from a region near the X-point toward the inner divertor target. The principal features of the image have been successfully re-produced with forward modelling techniques, by simply applying two physical assumptions. Firstly, that light is emitted with uniform brightness along field lines. Secondly, assuming a simple distribution of field lines consistent with where the fluctuations appear in the tangency plane. This produces a 3D light distribution, through which line integrals can be calculated to simulate a camera image. The figure to the right of Figure 2 shows the results of such forward modelling calculations for filaments in the main SOL (blue), fluctuations near the separatrix (gold) and in the PFR (green). Key features in the images are reproduced, for example the filaments appearing brighter at the tangency plane and that the filaments in the main SOL appearing sharper in the far-field.

3. Correlations in the PFR

The camera viewing geometry, imaging the divertor volume, means that viewing chords that are tangential to flux surfaces in the PFR of the inner divertor leg also detect light being emitted from the outer divertor leg. Although camera measurements are normally strongly weighted to the region where the camera viewing cords are tangential, contributions to the measured signal from other regions of the plasma can be a source of uncertainty regarding where the detected light was emitted. Furthermore, uncertainties in equilibrium reconstruction are a concern in definitively identifying the location of the filaments. To

ascertain whether the observed fluctuations are genuinely due to processes local to the PFR, the correlation of light fluctuations was investigated.

The cross-correlation between two discrete time-series data, x and y (in arbitrary units), with mean values $\bar{x}$ and $\bar{y}$, for a given lag time L (integer; multiples of data acquisition time intervals) is calculated using [8]:

$$P_{xy}(L)=\begin{cases}\dfrac{\sum_{k=0}^{N-|L|-1}\left(x_{k+|L|}-\bar{x}\right)\left(y_k-\bar{y}\right)}{\sqrt{\left[\sum_{k=0}^{N-1}\left(x_k-\bar{x}\right)^2\right]\left[\sum_{k=0}^{N-1}\left(y_k-\bar{y}\right)^2\right]}} & \text{for } L<0 \\ \dfrac{\sum_{k=0}^{N-L-1}\left(x_k-\bar{x}\right)\left(y_{k+L}-\bar{y}\right)}{\sqrt{\left[\sum_{k=0}^{N-1}\left(x_k-\bar{x}\right)^2\right]\left[\sum_{k=0}^{N-1}\left(y_k-\bar{y}\right)^2\right]}} & \text{for } L\geq 0\end{cases}$$

The cross-correlation between pairs of pixels was investigated using data 1,000 frames to investigate how fluctuations that occur in a given part of the image correlate with fluctuations elsewhere. A sample of raw data from two well correlated pixels separated by ~30cm in major radius is shown in Figure 3. The pixel indicated at the centre of the solid blue ellipse in Figure 4 indicated by a white cross was cross-correlated with the a subset of the pixels that detected light from the plasma, which reveals a second region of correlation ~30cm away from the pixel of interest (measured in the camera tangency plane). The locations of the correlated regions are insensitive to the baseline subtraction method applied to the raw data, and are also detected in the raw data without a baseline subtraction applied. An outline of the region of good local correlation to the pixel of interest (shown in solid blue in Figure 4) was mapped along the magnetic field back to the camera tangency plane, approximately one toroidal transit around the torus, which overlays well with the second correlated region (shown in dashed blue). This indicates that the two regions are well correlated because they are connected to the same field lines within the PFR. This provides strong evidence to suggest that these fluctuations in the camera data are genuinely in the PFR. In general, it is observed that fluctuations in the inner and outer leg private flux regions are correlated. The magnetic

mapping of correlated regions in the PFR suggests that fluctuations in the PFR near the X-point should correlate with fluctuations in both inner and outer legs, however, it is difficult to observe the fluctuations in the outer leg experimentally due to the strong magnetic shear in this region and line integration effects resulting in a significant contribution to the signal from the SOL of the outer leg.

4. Filament Propagation in the PFR

The filaments appear to move in the camera image plane along the inner divertor leg, originating from a given location in the leg and moving toward the inner target plate, as shown in Figure 5. The analysis of the camera data carried out so far does not suggest the filaments originate preferentially from a given location along the divertor leg. Whilst the precise nature of the motion of the filaments is uncertain due to the helical field line geometry, the conventional limits of assumed poloidal or toroidal motion give the estimated propagation velocity and angular velocity respectively as 1-2km/s or 10-20krad/s as confirmed by the data shown in Figure 5, where each pixel corresponds to approximately 6mm in the tangency plane. As the filaments propagate toward the inner target, the filaments eject plasma away from the separatrix.

5. Summary and Discussion

Results from fast imaging of light fluctuations in the MAST divertor are presented, suggesting that there are three types of field-aligned fluctuations native to the divertor region: filaments in the SOL originating upstream that are highly sheared by the X-point, small centimetre-scale fluctuations near the separatrix and filaments in the private flux region. Correlation analysis of the data from the PFR shows that fluctuations occurring in one part of the image are correlated with fluctuations occurring elsewhere in the PFR, and that these regions are connected by field lines. Tracking the filaments in the image plane for the H-mode period considered shows a motion equivalent to either a toroidal angular velocity of 10-20krad/s, or a poloidal velocity of 1-2km/s. These observations are in broad agreement with velocity measurements made of inter-ELM filaments on MAST in the SOL [9].

The data suggests that intermittent transport, in the form of filaments, plays a role in cross-field transport in the PFR in comparison with the well-known SOL behaviour. The role these filaments play in determining the time-averaged particle and heat fluxes to divertor PFCs is an open question, and will be investigated

further with analysis of experimental data, from cameras and other diagnostics, and also input from modelling. However, recent observations of radiated power fluctuations in the inner leg at the onset of detachment in AUG [10] suggest that intermittency in the inner leg could play a role in a several observed phenomena in the divertor.

Acknowledgements

This work was part-funded by the RCUK Energy Programme [grant number EP/I501045] and by the European Union's Horizon 2020 research and innovation programme. To obtain further information on the data and models underlying this paper please contact PublicationsManger@ccfe.ac.uk. The view and opinions expressed herein do not necessarily reflect those of the European Commission. We acknowledge the use made of the Photron SA1.1 which was borrowed from the EPSRC (Engineering and Physical Sciences Research Council) Engineering Instrument Pool.

References

[1] T. Eich et al., *Phys. Rev. Lett* **107** 21, 215001 (2011)

[2] R. J. Goldston, *Nucl. Fusion* **52** (2012) 013009

[3] I Garcia-Cortés et al., PPCF **38** (1996) 2051-2062

[4] B. D. Dudson, Ph.D thesis

[5] J. Terry et al., J. Nucl. Mater., **390**-**39** (2009) 339-342

[6] M. V. Umansky et al., J. Nucl. Mater 337-339 (2005) 266-270

[7] R. H. Cohen, D. D. Ryutov, Contrib. Plasma. Phys, 46 (2006) 678-684

[8] Exelis Visual Information Solutions. 2010. IDL user guide. Boulder, Colorado: Exelis Visual Information Solutions.

[9] N Ben Ayed et al Plasma Phys. Control. Fusion **51** (2009) 035016

[10] S. Potzel et al., J. Nucl. Mater., **438** (2013) 285-290

Figure Captions

Figure 1: Left: illustration of the MAST divertor volume imaged by the camera. Right: a raw image acquired by the camera from an inter-ELM H-mode period of a lower single-null discharge, showing the X-point and inner and outer divertor legs.

Figure 2: Left: background-subtracted image from Figure 1, showing fluctuations in the SOL, near the separatrix and in the PFR. The equilibrium separatrix mapped to the camera tangency plane has been overlaid as a red contour. Right: results of forward modelling calculations of the divertor fluctuations, calculated by calculating line integrals through field lines that correspond to the fluctuations observed in the left image.

Figure 3: A sample of raw data from two highly correlated pixels within the private flux region. The red trace is taken from a pixel viewing the PFR of the inner leg and the blue trace is taken from a pixel viewing the PFR of the outer leg.

Figure 4: Results of correlation analysis, where one pixel (indicated by a white cross) is cross-correlated with the pixels that view the plasma, over 1,000 frames (8ms total duration). The solid blue ellipse is fit around the region of local correlation for that pixel. This region is mapped along the magnetic field to the tangency plane to produce the ellipse shown in dashes, which corresponds to the position of the second correlated region near the outer leg.

Figure 5: Background-subtracted images showing the propagation of a filament in the PFR, starting near the X-point at the upper right part of the left images, propagating toward the inner divertor target at the bottom left as time advances.

Figures

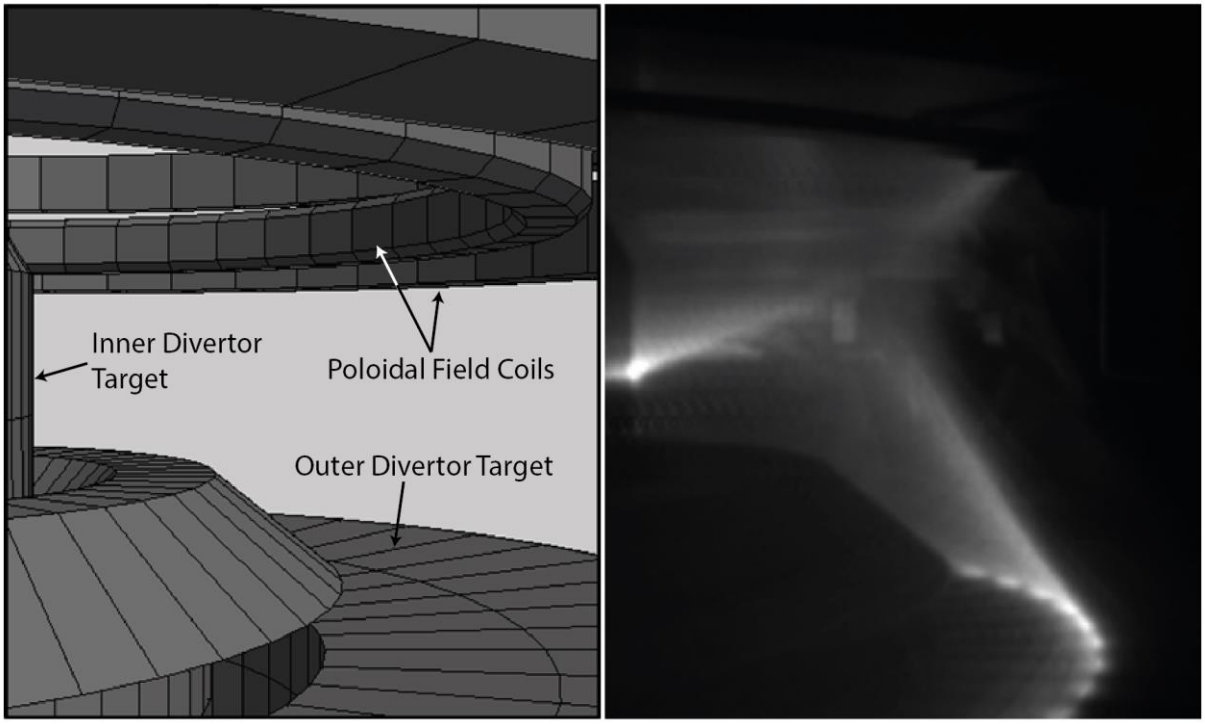

Figure 1

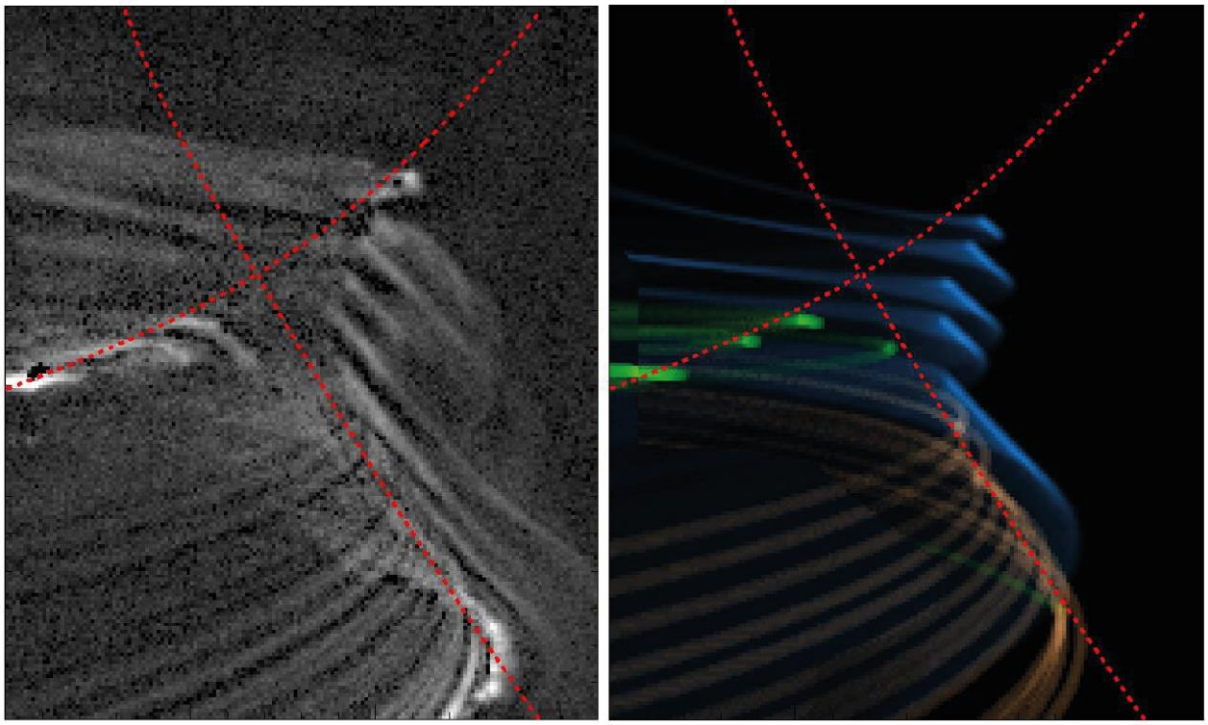

Figure 2

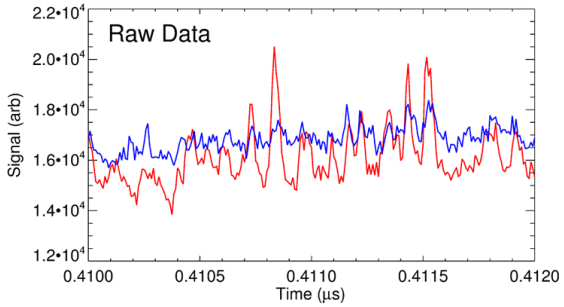
Raw Data
Signal (arb)
Time (μs)
2.2•10^4
2.0•10^4
1.8•10^4
1.6•10^4
1.4•10^4
1.2•10^4
0.4100
0.4105
0.4110
0.4115
0.4120

Figure 3

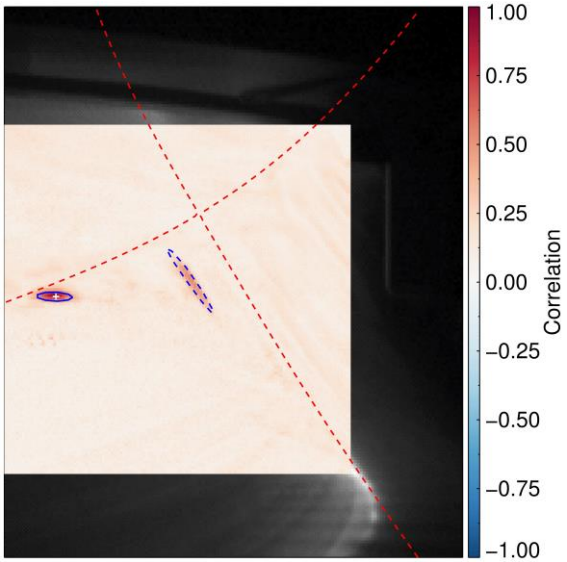

Figure 4

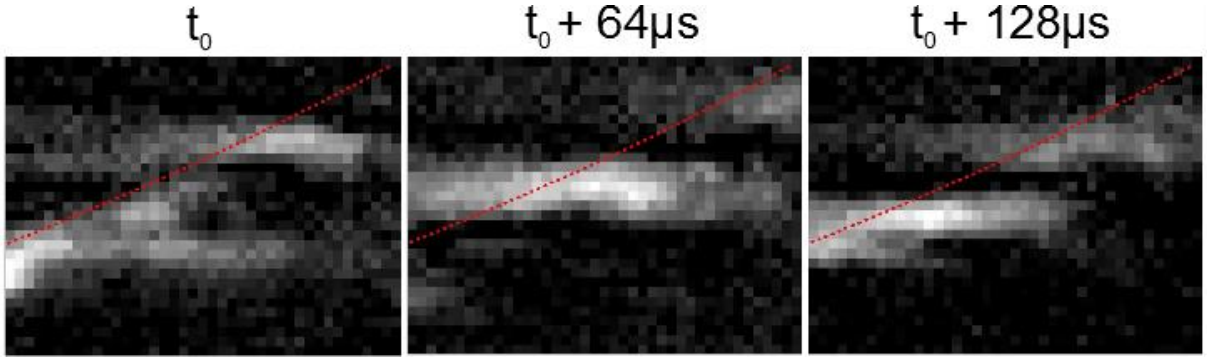

Figure 5